Materials Science-Poland, *Vol. 28*, *No. 1*, *2010*

Fabrication of core-shell Ge–GeO_2 nanoneedles

L.Z. PEI[1], H.S. ZHAO[1], W. TAN[2], H.Y. YU[1], Q.-F. ZHANG[1*]

[1]School of Materials Science and Engineering, Institute of Molecular Engineering and Applied Chemistry, Anhui University of Technology, Ma'anshan, Anhui 243002, P.R. China

[2]Henkel Huawei Electronics Co. Ltd., Lianyungang, Jiangsu 222006, P.R. China

Core-shell Ge–GeO_2 nanoneedles were prepared by a hydrothermal deposition using Ge and GeO_2 as starting materials. The samples were characterized by scanning electron microscopy, energy dispersive X-ray spectroscopy, transmission electron microscopy and high-resolution transmission electron microscopy. The results demonstrate that the length of the samples with typical needle structure is higher than 10 μm. The obtained nanoneedles are composed of single crystalline Ge with diamond cubic structure and amorphous oxide outer layers. An explanation of the formation and growth of Ge nanoneedles is proposed, and is based on the metallic-catalyst vapour-liquid-solid and oxide-assisted growth mechanisms.

Keywords: *Ge–GeO_2 nanoneedles; hydrothermal deposition; characterizations*

1. Introduction

Germanium is an important semiconductor with a direct band gap of 0.8 eV and an indirect band gap of 0.66 eV. Recently, interest in germanium has intensified as the migration from silicon to other materials is contemplated for enhanced functionality of future transistors for logic and other functions. Compared with bulk silicon, bulk germanium offers several advantages such as higher intrinsic carrier mobilities, promising faster switching and higher frequency devices, higher intrinsic carrier concentrations, larger bulk excitonic Bohr radii (24.3 nm for Ge versus 4.7 nm for Si), etc. Also, compatibility of germanium with the group of III–V materials (e.g., good lattice matching with GaAs) and optical properties of germanium oxide allow fabrication of radical integrated optoelectronic circuitry designs [1, 2]. Therefore, the one-dimensional nanoscale materials of Ge have many potential applications such as in nanoscale probes, nanoscale electron devices and nanoscale sensors. Ge nanowires and nanoneedles with core-shell structure are two kinds of one-dimensional solid forms of Ge. Ge nanowires with uniform diameter can be prepared easily by the laser ablation method [3], chemical vapour deposition (CVD) [4, 5], thermal evaporation [6], the

*Corresponding author, email: zhangqf@ahut.edu.cn

template method [7, 8] and the supercritical fluid method [9, 10]. In comparison with semiconductor Ge nanowires, Ge nanoneedles are also particularly interesting because their tips exhibit a sharp curvature. Due to their tapered shapes, nanoneedles can potentially be applied as probe tips with high spatial resolution but any damage to probed microstructures should be minimal. They can also be used as field-emission tips with outstanding field enhancement factors [11–13]. Unlike nanowires of uniform diameter, nanoneedles with sharp tips are difficult to prepare. Only a few kinds of semiconductor nanoneedles have been reported, such as silicon [14, 15], ZnO [13, 16, 17], Se [18] and ZnSe [19]. Therefore, the fabrication of Ge nanoneedles is still challenging. In this paper, we report a simple hydrothermal deposition route for the preparation of Ge nanoneedles with Ge–GeO_2 core-shell structure. The products have been characterized by scanning electron microscopy (SEM), energy dispersive X-ray spectroscopy (EDS), transmission electron microscopy (TEM), selected area electron diffraction (SAED) and high-resolution transmission electron microscopy (HRTEM). The growth mechanism of Ge–GeO_2 core-shell nanoneedles is also discussed.

2. Experimental

The preparation of Ge–GeO_2 core-shell nanoneedles was performed in an autoclave. The autoclave is composed of stainless steel (1Cr18Ni9Ti) with maximum pressure of 22 MPa, maximum temperature – 500 °C, volume 1000 cm^3, power – 1.5 kW and stirring velocity of the stirrer from 0 to1000 rpm. 2 wt. % Ge and GeO_2 (purity of both $\geq$ 99.99%) were mixed with 48 cm^3 of distilled water. The mole ratio of Ge and GeO_2 was 1:1. Then the mixture was placed in the autoclave. The copper sample of the dimensions 4 × 2 cm^2 was cleaned in distilled water for 10 min using supersonic wave apparatus in order to ensure the cleanliness in the surface of the copper substrate. Then, the latter was fixed in the stainless steel bracket in the centre of the autoclave. After the autoclave was sealed safely, it was heated to 480 °C, subject to a pressure of 9–10 MPa, and stirred at the rate of 100 rpm. The constant temperature and pressure were maintained for 24 h. Subsequently the autoclave was cooled in air. Finally, the copper substrate with bulk deposit was obtained after the experiment. SEM and TEM confirmed that the product were Ge–GeO_2 core-shell nanoneedles.

Scanning electron microscopy observations were performed using a JEOL JSM5410 scanning electron microscope with the 15 kV accelerating voltage. Chemical analysis was performed with an energy dispersive X-ray spectroscope attached to the scanning electron microscope. The product was mechanically scrapped from the copper substrate. Transmission electron microscopy and high-resolution transmission electron microscopy samples were prepared by putting several drops of solution containing nanoneedles onto a standard copper grid with a porous carbon film after the nanoneedle samples had been dispersed in distilled water and treated for about 10 min using a supersonic wave apparatus. Transmission electron microscopy and high-resolution transmission electron microscopy observations were performed using

a JEOL JEM-2100 transmission electron microscope operating with 1.9 Å point-to-point resolution, and a 200 kV accelerating voltage, equipped with a GATAN digital photography system.

3. Results and discussion

SEM observations show an abundant number of cluster-like nanoneedles on the substrate. In Figure 1, typical SEM images of the nanoneedles under various magnifications are seen. It was found that the substrate is uniformly covered by pure nanoneedle structures.

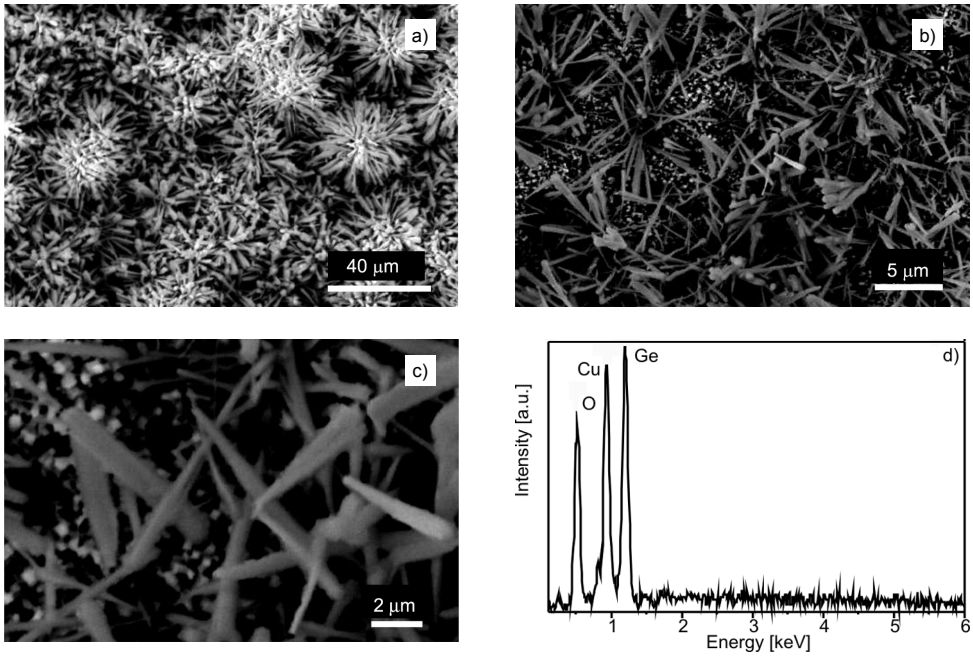

Fig. 1. General SEM images of the obtained nanoneedles with various magnifications (a)–(c) and the corresponding EDS spectra of the nanoneedles (d)

The length of each nanoneedle exceeds 10 μm. The diameter of each nanoneedle is continuously smaller towards one end, and the average diameter of needle tips is lower than 1 μm. Most nanoneedles have sharp tips and smooth surfaces, showing that their morphology is similar to that of other kinds of nanoneedles [14–19]. In order to determine the components of the obtained nanoneedles, the products are analyzed with an EDS spectrometer equipped with the SEM (Fig. 1d). According to the EDS data, the obtained nanoneedles are composed of Ge, O and Cu. No other elements are observed from the EDS spectroscopy.

Figure 2a shows a typical TEM image of the nanoneedles, which is similar to the SEM results. The corresponding SAED is shown in the inset of Fig. 2a. The SAED displays typical diffraction patterns of the {111}, {220} and {311} planes, which indicate that the nanoneedles are in a single crystalline form with a cubic diamond phase. Figure 2b is a typical high magnification TEM image of a single nanoneedle, revealing a sharp tip.

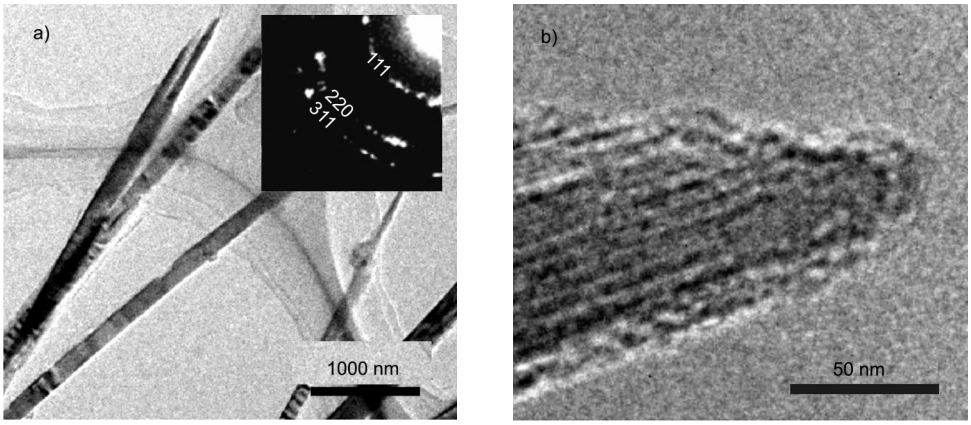

Fig. 2. General TEM image of the sample (a), the inset is the corresponding SAED pattern, and typical TEM image at the tip of a single nanoneedle (b)

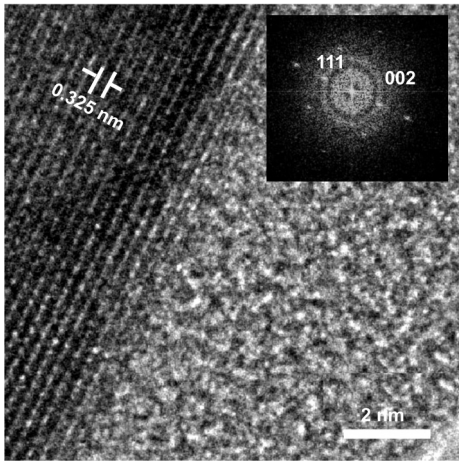

Fig. 3. HRTEM image of the sample, the inset is the corresponding diffraction pattern obtained by fast Fourier transformation (FET)

Figure 3 shows the HRTEM image of a single nanoneedle. The core-shell structure can distinctly be observed and the outer layer is amorphous, measuring several dozen nanometres. The crystalline interplanar spacing is about 0.325 nm, according to the HRTEM measurement and the subsequent calculation using the software of a digital micrograph (Gatan Inc., Pleasanton, CA) applied to the HRTEM, matching well with the {111} plane of Ge. In addition, the HRTEM image further confirms that the nanoneedles are single crystalline. The two-dimensional lattice image further reveals

that the obtained nanoneedles consist of single crystalline Ge cores and amorphous GeO_2 shell. The corresponding diffraction pattern obtained by fast Fourier transformation (FET) is shown in the inset of Fig. 3. [111] is the growth direction of the nanoneedles which is similar to that observed for Ge nanowires [9, 10, 20, 21].

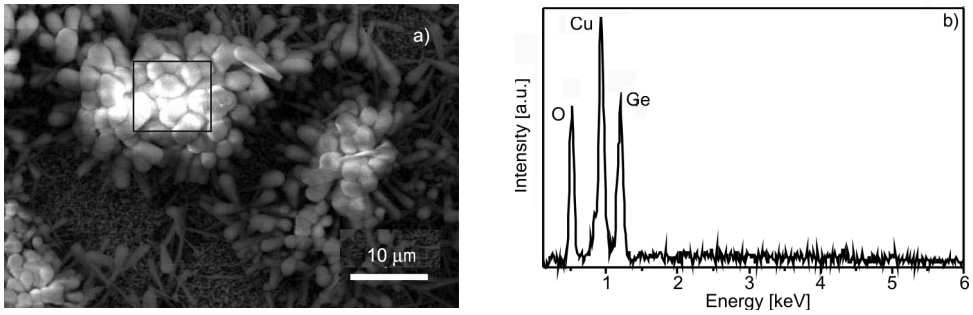

Fig. 4. SEM image of the tips of the nanoneedles (a) and the corresponding EDS spectra (designated by the black frame) (b)

The growth tips of the nanoneedles are shown in Fig. 4a. Sphere structures of various sizes are observed. The sphere structures are similar to the tips of catalyst alloys of other one-dimensional nanoscale materials, such as carbon nanotubes [22], silicon nanowires [23] and germanium nanowires [20] fabricated by metallic catalyst vapour-liquid-solid (VLS) growth methods. In addition, the corresponding EDS spectra (Fig. 4b) show that the sphere structures are composed of Ge, O and Cu. The content of Ge is obviously lower than that of Cu. The results show that the sphere structures at the tips are a kind of Cu/Ge/O catalyst alloy sphere. It is well known that the presence of solidified catalyst droplets of one-dimensional nanostructures is an evidence for the effective operation of the VLS mechanism, and the size of the droplet commonly governs the diameter of one-dimensional nanostructures [19]. Therefore, the formation of the Ge nanoneedles is believed to be very close to the metallic catalyst VLS growth mechanism. The increase in size of catalyst droplets during the growth probably results in the formation and growth of Ge nanoneedles. However, the peculiar needle-like structure of our grown products indicates that the growth of the nanoneedles does not seem to be governed solely by the VLS mechanism, although Cu/Ge/O catalyst spheres do exist. The Cu/Ge/O catalyst droplets contain a significant amount of oxide. It is also well known that it plays a vital role in the formation and growth of one-dimensional nanomaterials, such as silicon nanowires and germanium nanowires. The formation and growth process can be explained by the oxide-assisted growth (OAG) mechanism proposed by Lee et al. [6, 24–27]. Therefore, oxide is also considered to play an important role in the formation and growth of the nanoneedles. Both mechanisms show an approximately equal probability of occurrence. The possible growth mechanism is proposed below.

The starting materials, Ge and GeO_2 are a stable monoatomic element and oxide in a normal atmospheric environment at room temperature. The melting points of Ge and

GeO_2 are 937.4 °C and 1115 °C, respectively. Therefore, the starting materials are difficult to be gasified, reacting each other under the ambient atmospheric pressure and at experimental temperature under consideration here. The deposition process, however, was conducted under the pressure of 9–10 MPa at the temperature of 480 °C, which is higher than the critical temperature of water (374 °C) [28]. Therefore, the experiments are considered to be carried out under the supercritical hydrothermal conditions. Supercritical water has sufficient density to dissolve materials, a higher diffusivity than in liquid state, low viscosity facilitating mass transport, and high compressibility allowing easy changes in density and dissolving power [29, 30]. Thus the supercritical hydrothermal conditions may play an essential role in the reaction and gasification of Ge and GeO_2. The hydrothermal pressure can also enhance the reaction according to chemical reaction theory. Therefore, the reaction of Ge and GeO_2 should proceed, forming GeO under the present supercritical hydrothermal conditions.

GeO is an unstable compound and disproportionates into Ge atoms and GeO_2 molecules forming Ge/GeO_2 nanoscale clusters. The nanoclusters are suspended in the supercritical hydrothermal environment under continuous stirring. The melting temperature of these nanoclusters may be reduced due to their nanoscale size and the effect of the supercritical hydrothermal environment [28–30]. The nanoclusters might be liquid-like, in a semi-molten or molten state. They deposit onto the substrates continuously as the air flows into the autoclave. The supercritical hydrothermal conditions also enhance the oxidation and melting of Cu on the surface of the substrate. Cu reacts with O in the hydrothermal environment to form a large amount of molten Cu oxide nanoclusters on the surface of the substrate. The Cu/Ge/O catalyst droplets form from the molten nanoscale Cu oxide and from deposited Ge, Ge oxide nanoscale clusters. Therefore, the formation and growth of Ge nanoneedles are believed to follow simultaneously the metallic-catalyst VLS and OAG growth mechanisms.

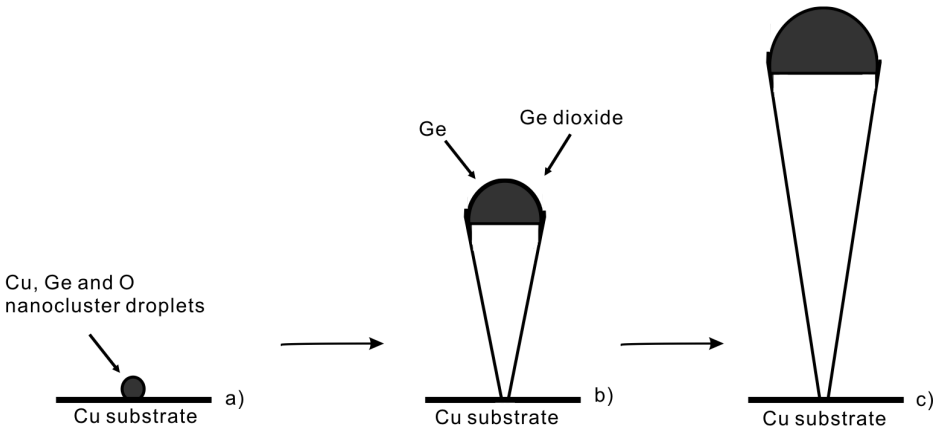

Fig. 5. The proposed metallic catalyst VLS and OAG growth scheme of the nanoneedles: a) the nucleation of the Cu/Ge/O catalyst droplets, b) the growth of the nanoneedles according to the metallic catalyst VLS and OAG growth mechanism, c) the final formation of the nanoneedles

Figure 5 shows the metallic-catalyst VLS and OAG growth scheme of the core-shell nanoneedles. The can be divided into the nucleation and growth of liquid Cu/Ge/O catalyst droplets. The Cu/Ge/O catalyst droplets form from the molten nanoscale Cu oxide and are deposited as Ge, Ge oxide nanoscale clusters (Fig. 5a). Liquid metallic catalyst droplets limit the diameter of the Ge nanoneedles. With the further absorption of Ge atoms and GeO_2 molecules into the droplets from the environment, the Ge atoms are in the supersaturation state and move across the interface between the catalyst and the nanoneedles, thereby resulting in the growth of Ge nanoneedles (Figs. 5b, c). According to the VLS mechanism, the diameter of one-dimensional nanomaterials depends on the size of the nanoclusters that are formed initially [31]. The relation between the nanocluster diameters and the ambient gas pressure is governed by the inertia fluid model proposed by Yoshida et al. [32], which is as follows:

$$d \propto p^n, \quad n = \frac{1}{3} \tag{1}$$

Here d is the diameter of the catalyst alloy nanoclusters, p is the ambient gas pressure. Therefore, the diameter of the Cu/Ge/O nanoclusters at the top of one-dimensional Ge nanoscale structures increases as the ambient gas pressure p increases to 10 MPa. Finally, special nanoneedle structures with sharp tips form. In addition, similar to the metallic catalyst VLS growth mechanism, liquid-like Ge oxide in the Ge/Cu/O nucleus plays also the role of metallic catalysts, according to the OAG mechanism. The Ge/Cu/O nucleus continuously absorbs Ge atoms and Ge oxide molecules from the atmosphere and undergoes recrystallization with phase separation into Ge and Ge oxide. Crystallized Ge stays inside and amorphous Ge oxide diffuses towards the nanoneedle surface. Subsequently, an amorphous GeO_2 shell will be formed [6]. From the thermodynamic viewpoint, recrystallization with phase separation is the result of free energy minimization of the system [6]. The crystalline structure will extend continuously in the axial direction, due to the rapid deposition of nanoclusters at the tip resulting in the growth of the nanoneedles. Therefore, the obtained nanoneedles with the single crystalline Ge cores are covered with oxide outer layers measuring several dozen nanometres.

4. Conclusions

Nanoneedles with Ge–GeO_2 core-shell structure longer than 10 μm have been synthesized by a simple hydrothermal deposition using Ge and GeO_2 as the starting materials. The obtained nanoneedles are covered with oxide outer layers measuring several dozen nanometres, and have single crystalline Ge cores with diamond cubic structure. The nanoneedle diameters become smaller towards one end: the average diameter of the tips is lower than 1 μm. Most needles have sharp tips and smooth surfaces. The formation and growth of the nanoneedles are believed to follow a similar profile to that of the metallic-catalyst VLS and OAG.

Acknowledgements

This work was supported by the National Basic Research Program of China (973 Program, 2008CB617605) and the Program for New Century Excellent Talents in University of China NCET-06-0556).

References

[1] NGUYEN P., NG H.T., MEYYAPPAN M., Adv. Mater., 17 (2005), 549.
[2] WANG L., WANG X.S., TANG J.C., CUE N., Mater. Charact., 48 (2002), 189.
[3] MORALS A.M., LIEBER C.M., Science, 279 (1998), 208.
[4] WANG D., DAI H., Angew. Chem. Int. Ed., 41 (2002), 4783.
[5] DAILEY J.W., TARACI J., CLEMENT T., SMITH D.J., DRUCKER J., PICRAUX S.T., J. Appl. Phys., 96 (2004), 7556.
[6] ZHANG Y.F., TANG Y.H., WANG N., LEE C.S., BELLO I., LEE S.T., Phys. Rev. B, 61 (2001), 4518.
[7] COLEMAN N.R.B., RYAN K.M., SPALDING T.R., HOLMES J.D., MORRIS M.A., Chem. Phys. Lett., 343 (2001), 1.
[8] HAN W.Q., WU L.J., ZHU Y.M., STRONGIN M., Microsc. Microanal., 11 (2005), 1506.
[9] HANRATH T., KORGEL B.A., J. Am. Chem. Soc., 124 (2002), 1424.
[10] HANRATH T., KORGEL B.A., Small, 1 (2005), 717.
[11] KIM P., LIEBER C.M., Science, 286 (1999), 2148.
[12] ZHU Y.W., ZHANG H.Z., SUN X.C., FENG S.Q., XU J., ZHAO Q., XIANG B., WANG R.M., Appl. Phys. Lett., 83 (2003), 144.
[13] PARK W.I., YI G.G., KIM M., PENNYCOOK S.J., Adv. Mater., 14 (2002), 1841.
[14] CHEN Y.W., JIANG S.H., SHAO B.X., WANG W., WANG R.C., J. Electron Mater., 37 (2008), 176.
[15] JUNG S., YOO J., KIM Y., KIM K., DHUNGEL S.K., YI J., Mater. Sci. Eng. C, 26 (2006), 813.
[16] LEE W., JEONG M.C., KIM M.J., MYOUNG J.M., Phys. Lett., 370 (2007), 345.
[17] ZHANG J., YANG Y.D., JIANG F.H., LI J.P., Physica E, 27 (2005), 302.
[18] XIONG S.L., XI B.J., WANG W.Z., WANG C.M., FEI L.F., ZHOU H.Y., QIAN Y.T., Cryst. Growth Des., 6 (2006), 1711.
[19] FU H.Z., LI H.Y., JIE W.Q., YANG L., J. Cryst. Growth, 289 (2006), 440.
[20] MATHUR S., SHEN H., SIVAKOV V., WERNER U., Chem. Mater., 16 (2004), 2449.
[21] LU X.M., FANFAIR D.D., JOHNSTON K.P., KORGEL B.A., J. Am. Chem. Soc., 127 (2005), 15718.
[22] JIANG Y., WU Y., ZHANG S.Y., XU C.Y., J. Am. Chem. Soc., 122 (2000), 12383.
[23] FENG S.Q., YU D.P., ZHANG H.Z., BAI Z.G., DING Y., J. Cryst. Growth, 209 (2000), 513.
[24] MA D.D.D., LEE C.S., AU F.C.K., TONG S.Y., LEE S.T., Science, 299 (2003), 1874.
[25] LEE S.T., ZHANG Y.F., WANG N., TANG Y.H., BELLO I., LEE C.S., CHUNG Y.W., J. Mater. Res., 14 (1999), 4503.
[26] LEE S.T., WANG N., ZHANG Y.F., TANG Y.H., MRS Bull., 24 (1999), 36.
[27] ZHANG Y.F., TANG Y.H., WANG N., LEE C.S., BELLO I., LEE S.T., J. Cryst. Growth, 197 (1999), 136.
[28] CUMMINGS P.T., COCHRAN H.D., SIMONSON J.M., MESMER R.E., KARABORNI S., J. Chem. Phys., 94 (1991), 5606.
[29] TANG Y.H., PEI L.Z., CHEN Y.W., GUO C., Phys. Rev. Lett., 95 (2005), 116102.
[30] PEI L.Z., TANG Y.H., ZHAO X.Q., CHEN Y.W., GUO C., J. Appl. Phys., 100 (2006), 046105.
[31] YANG Y.H., WU S.J., CHIU H.S., LIN P.I., CHEN Y.T., J. Phys. Chem. B, 108 (2004), 846.
[32] YOSHIDA T., TAKEYAMA S., YAMADA Y., MUTOCH K., Appl. Phys. Lett., 68 (1996), 1772.

Received 8 October 2008
Revised 9 November 2009